# Magnetically Recoverable, Thermostable, Hydrophobic DNA/Silica Encapsulates and Their Application as Invisible Oil Tags

**Michela Puddu, Daniela Paunescu, Wendelin J. Stark, and Robert N. Grass***

Functional Materials Laboratory, ETH Zurich, Vladimir-Prelog-Weg 1, 8093 Zurich, Switzerland

**ABSTRACT** A method to encapsulate DNA in heat-resistant and inert magnetic particles was developed. An inexpensive synthesis technique based on co-precipitation was utilized to produce $Fe_2O_3$ nanoparticles, which were further functionalized with ammonium groups. DNA was adsorbed on this magnetic support, and the DNA/magnet nanocluster was surface coated with a dense silica layer by sol–gel chemistry. The materials were further surface modified with hexyltrimethoxysilane to achieve particle dispersibility in hydrophobic liquids. The hydrodynamic particle sizes were evaluated by analytical disc centrifugation, and the magnetic properties were investigated by vibrating sample magnetometry. The obtained nanoengineered encapsulates showed good dispersion abilities in various nonaqueous fluids and did not affect the optical properties of the hydrophobic dispersant when present at concentrations lower than $10^3$ $\mu$g/L. Upon magnetic separation and particle dissolution, the DNA could be recovered unharmed and was analyzed by quantitative real-time PCR and Sanger sequencing. DNA encapsulated within the magnetic particles was stable for 2 years in decalin at room temperature, and the stability was further tested at elevated temperatures. The new magnetic DNA/silica encapsulates were utilized to developed a low-cost platform for the tracing/tagging of oils and oil-derived products, requiring 1 $\mu$g/L = 1 ppb levels of the taggant and allowing quantification of taggant concentration on a logarithmic scale. The procedure was tested for the barcoding of a fuel (gasoline), a cosmetic oil (bergamot oil), and a food grade oil (extra virgin olive oil), being able to verify the authenticity of the products.

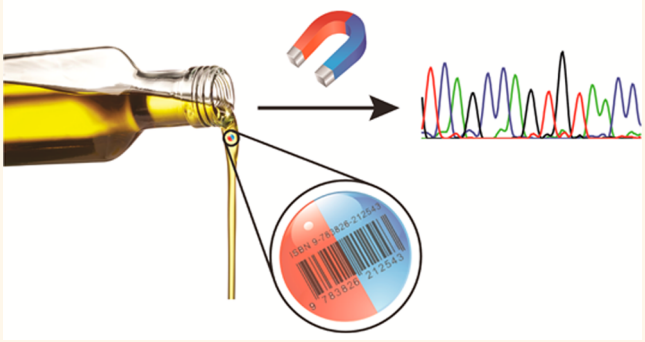

**KEYWORDS:** counterfeit · barcode · nucleic acid · TEOS · qPCR

Today, adulteration extends to almost all types of products. Fuels, high-value cosmetic oils and foodstuff (such us extra virgin olive oil), medicines, and other chemicals are routinely counterfeited to produce illegitimate profit. Fuel stealing or illegal treading is a real problem in many countries, being responsible for huge money losses for governments.[1,2] For this reason, several oil authentication programs have been promoted. Extra virgin olive oil adulteration with cheaper oil has become more frequent in recent years.[3,4] Authenticity determination of olive oil product is fundamental for both trader interests and consumer health. Essential oils are expensive oils with a variety of cosmetic, therapeutic, and culinary uses which are also often adulterated to increase profit.[5] However, only pure products contain a full range of components in the right ratios, imparting unique aroma, cosmetic, and therapeutic properties that fake imitations cannot replicate.

Several tagging approaches have been proposed against adulteration, making use of imperceptible labels attached or integrated within products and identifiable by specific instruments and procedures. Besides being invisible, a product tag should be inert, resistant, and harmless. Additionally, it should not affect product properties and should be cheap and easily detected. Tagging technologies include magnetic inks,[6] fluorescent labels,[7] photochromic and thermochromic inks,[8] isotopic tracers,[9] and Raman-active components.[10] Polypeptides[11] and nucleic acids[12–14] have also

* Address correspondence to robert.grass@chem.ethz.ch.

Received for review December 13, 2013 and accepted February 25, 2014.

**Published online February 25, 2014**
**10.1021/nn4063853**

been used as taggants. Above all, DNA offers unique opportunities in this field, supported by mature DNA synthesis and analysis procedures.

Nucleic acids are Nature's method to store and transmit instructions. Double helix conformation and stability allow DNA to accomplish this vital function. Since DNA-related technologies were established, several artificial DNA structures for a broad range of applications have been designed.[15−23] The use of DNA codes has also been developed: DNA barcoding is now a well-known strategy to identify biological species, as DNA fingerprinting is used to prove the identity of people (paternity test, forensics, victim recognition) and the biological origin of foodstuff.[3] Instead of using natural occurring genomic sequences, artificial DNA with a unique sequence can also be introduced into goods to be marked.[12−14] In this way, identification of any branded product becomes possible.

The idea of writing, storing/carrying, and retrieving nongenetic information on DNA is powerful.[14,24−28] However, incredible capabilities of DNA as Nature's storage system also arise from the ability of organisms to repair DNA when lesions occur. DNA stability *per se* is limited[29] because it can be damaged by metabolic processes as well as by several environmental factors. When DNA is used as information storage/carrier outside living organisms (an idea dating back about 20 years), there is lack of repairing processes and DNA can be severely damaged. To avoid its degradation and preserve its integrity DNA has to be preventively protected. While good protection against enzymatic degradation can be achieved by DNA complexation with positively charged molecules/particles,[30,31] or encapsulation in polymeric capsules,[32] prevention of damage produced by radiation, temperature fluctuations, chemical (*e.g.*, redox) exposure is more challenging. Several cold and dry storage strategies, eventually combined and improved by storage additives,[33,34] are used to store/transport DNA. Alternative solutions, such as DNA encapsulation into porous silica matrix[35,36] or within layered metal hydroxide,[24,25] have also been proposed.

In previous studies,[14,28] we have encapsulated ssDNA and dsDNA of various lengths in silica to produce radical-resistant and heat-resistant "synthetic fossils". These silica materials could be dissolved with fluoride comprising buffers (*i.e.*, buffered oxide etch, BOE) to recover intact DNA. This approach allows for a protection of DNA against chemical attack because it provides a physical barrier that completely isolates DNA from the external environment, a situation very similar to that in natural fossils.

For the recovery of analytes from solution, magnetic separation methods are currently applied in different areas of analytical chemistry because of the advantages offered in comparison to similar nonmagnetic techniques.[37−39] Therein, magnetic separation of analytes allows for better sample handling and upconcentration and is suitable for use in a variety of automated analytical procedures. Fast and easy recovery of magnetic particles, as well as the absence of sample volume limitations, results in their broad utilization in separation, identification, and quantification of several chemical and biological species. For these reasons, the use of magnetic biotechnology[22,23] for tracing/tagging is very attractive.[13,40]

In the present article, we present how the above-described concepts of DNA analytics, magnetic separation, and silica encapsulation can be combined to generate potent (read out at 1 ppb) and low-cost (0.02 ¢/L of product) tracers for the marking of oil-based items.

We tested our tagging/tracing technology with three model oils, a fuel oil (gasoline), a cosmetic/therapeutic oil (bergamot oil, used in perfumery and cosmetics), and a food grade oil (extra virgin olive oil), to scan a range of different oil types and present the applicability of the newly designed materials.

## RESULTS AND DISCUSSION

Iron oxide nanoparticles were produced by a conventional co-precipitation method under ambient conditions. Since maghemite and magnetite XRD patterns are nearly identical, the iron oxide form obtained could not be identified by this method. However, the aerobic synthesis conditions predicted formation of $\gamma$-$Fe_2O_3$.[41] The nanocrystallite size, calculated from the XRD pattern (Figure 1a) by means of the Scherrer formula, was estimated to be 12 nm.

Magnetization data (Figure 1b and Table 1) revealed soft magnetic behavior of the nanoparticles, with a saturation magnetization of 50 emu/g and nearly zero hysteresis, as shown by the inset of Figure 1b, indicating superparamagnetic properties.

Hydrodynamic size distribution of the produced $Fe_2O_3$ nanoparticles was obtained using an analytical photocentrifuge (LUMiSizer, see Supporting Information). The mean hydrodynamic particle size according to Stokes' law (calculated using a density of 5.6 g/cm$^3$) was 43 nm.

The $Fe_2O_3$ nanoparticles were reacted with *N*-trimethoxysilylpropyl-*N*,*N*,*N*-trimethylammonium chloride (TMAPS)[14,28,42] to have surface ammonium groups able to interact with negatively charged DNA (Figure 2). The surface functionalization of the iron oxide with TMAPS was studied by IR spectroscopy (Figure 3), by zeta-potential measurements, and by element microanalysis (Table 2).

DNA was readily adsorbed on the surface of the positively charged magnetic nanoparticles, as evidenced by the IR spectrum (Figure 3), the zeta-potential value (Table 2), and by Qubit (see Supporting

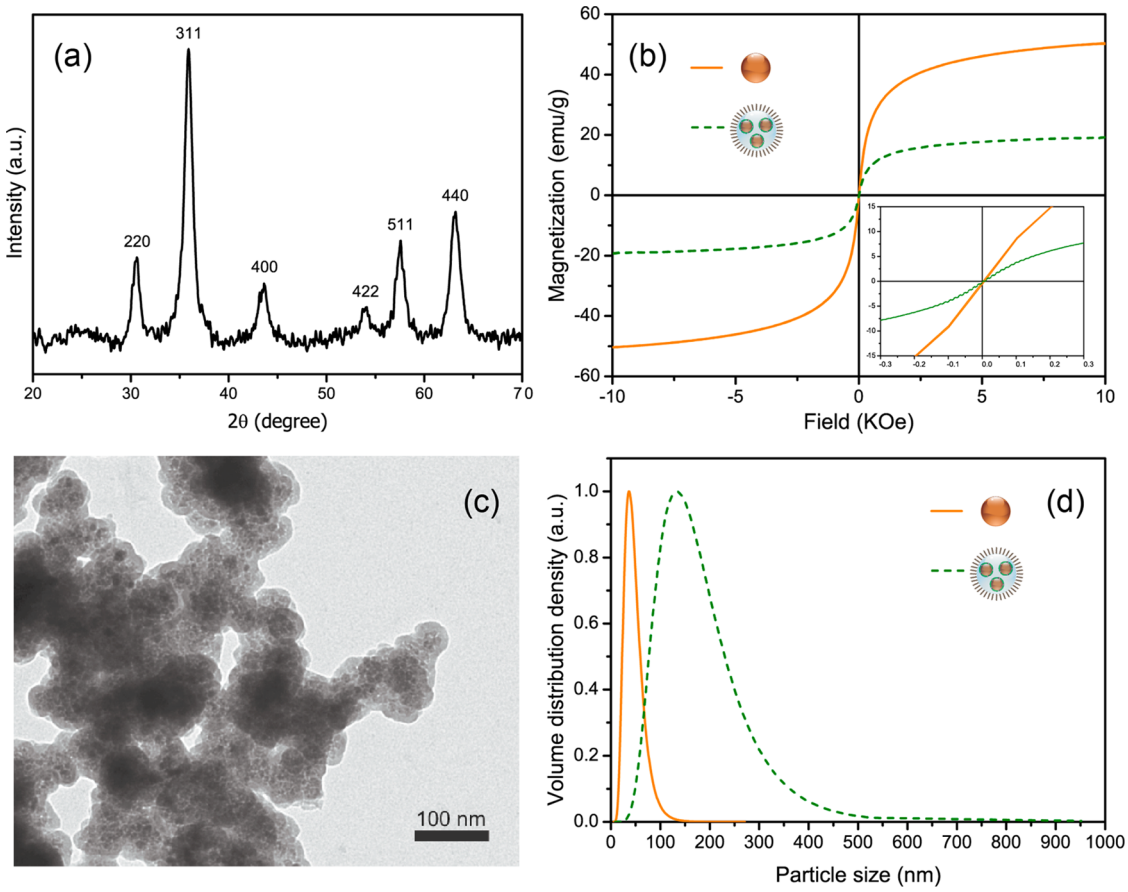


**Figure 1. (a) XRD pattern of $Fe_2O_3$ nanoparticles prepared by co-precipitation; (b) hysteresis loops of $Fe_2O_3$ nanoparticles (solid line) and of $Fe_2O_3$/TMAPS/DNA/$SiO_2$−$C_6$ particles (dashed line); (c) TEM micrograph of $Fe_2O_3$/TMAPS/DNA/$SiO_2$ particles; (d) particle size distributions of $Fe_2O_3$ nanoparticles in water (solid line) and of $Fe_2O_3$/TMAPS/DNA/$SiO_2$−$C_6$ particles in toluene (dashed line).**

**TABLE 1. Saturation Magnetization and Corresponding Coercivity and Remanence Data for Pristine $Fe_2O_3$ Particles and for $Fe_2O_3$/TMAPS/DNA/$SiO_2$−$C_6$**

| sample | magnetization (emu/g) | coercivity (Oe) | remanence (emu/g) |
|---|---|---|---|
| $Fe_2O_3$ | 50 | 2 | 0.2 |
| $Fe_2O_3$/TMAPS/DNA/$SiO_2$−$C_6$ | 19 | 2 | 0.1 |

Information) fluorometric quantitation (1.0 ± 0.5 $\mu$g DNA per mg of particles). In the following step, the particles were encapsulated in silica by using TMAPS as co-interacting species and tetraethoxysilane (TEOS) as a silica precursor,[14,28] as illustrated in Figure 2.

A dense silica coating was grown to ensure complete sealing of dsDNA adsorbed onto the iron oxide nanoparticles. Electron microscopy (Figure 1c) of the obtained nanostructured particles illustrates the maghemite cores embedded in the silica matrix. The presence of the nanometer thick silica coating was also verified by IR spectroscopy (Figure 3, band around 1090 $cm^{-1}$) and by zeta-potential measurements (Table 2). As expected, the presence of the $SiO_2$ shell reduced the magnetic performance of the material. The observed decrease of the saturation magnetization from 50 to 19 emu/g suggested the presence of ~60 wt % silica in the final material.

For read out of the presence and concentration of the tag, DNA has to be released from the particles. It is well-known that silica dissolves rapidly in fluoride-containing solutions (forming $SiF_6^{2-}$), but with the aid of some acidity, iron oxide is also attacked and dissolved in buffered fluoride solutions. Indeed, upon mixing aqueous suspensions of the particles with a buffered fluoride-containing solution (BOE, $F^-$ = 0.025 wt % in water, pH ~4), the silica top layer as well as the iron oxide cores were dissolved, and the DNA molecules were freed. The compatibility of dilute BOE solutions and DNA (DNA is not affected by $F^-$ ions) has previously been shown.[14,28] After dissolving $Fe_2O_3$ and $SiO_2$, the released DNA was amplified directly using a standard quantitative PCR protocol, without the need for purification prior to analysis. Even at the highest concentration of particles in water ($10^6$ $\mu$g/L = 1 g/L), the concentrations of the ionic species in the final PCR mix did not affect the polymerase efficiency ($SiF_6^{2-}$, $Fe^{2/3+}$, $NH_4^+$, and $F^-$ at calculated concentrations of ≤12, 2, 41, and 63 $\mu$g/mL, respectively). Figure 4 shows

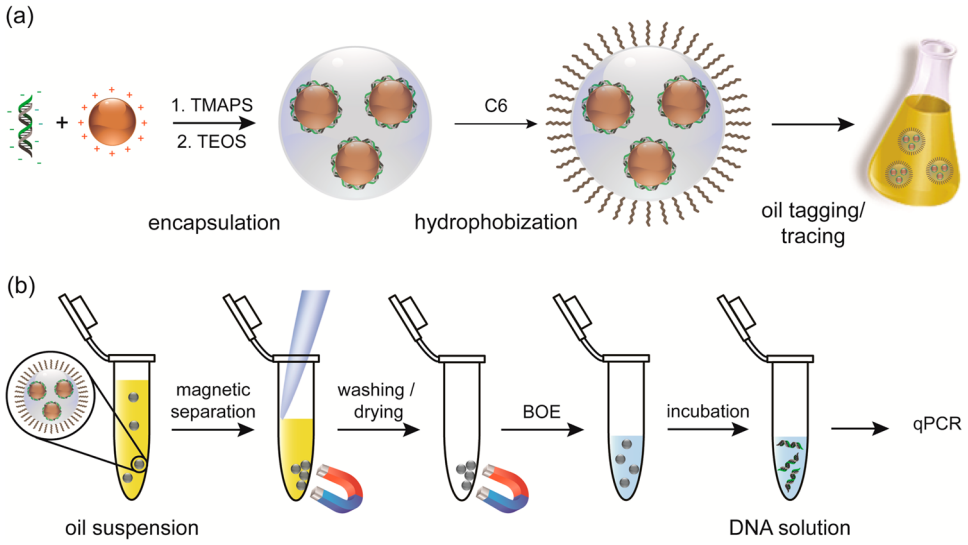


**Figure 2. (a) Synthesis of $Fe_2O_3$/TMAPS/DNA/$SiO_2$−$C_6$ particles and (b) analytic route of DNA recovery from oil particle suspensions and subsequent quantification by qPCR.**

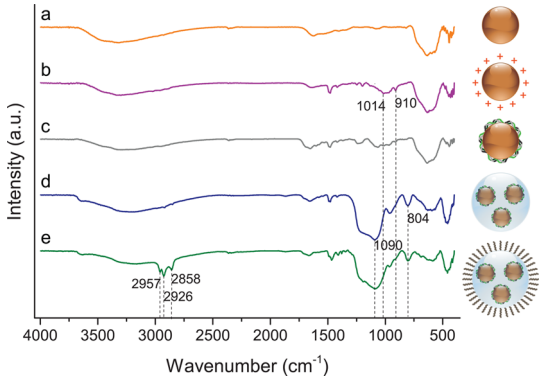


**Figure 3. IR spectra of (a) $Fe_2O_3$ nanoparticles, (b) $Fe_2O_3$/TMAPS, (c) $Fe_2O_3$/TMAPS/DNA, (d) $Fe_2O_3$/TMAPS/DNA/$SiO_2$, and (e) $Fe_2O_3$/TMAPS/DNA/$SiO_2$−$C_6$ particles.**

**TABLE 2. Zeta-Potential Data and Element Microanalysis for Carbon, Hydrogen, and Nitrogen**

| sample | C% | H% | N% | zeta-potential (mV) |
|---|---|---|---|---|
| $Fe_2O_3$ | 0.22 | 0.75 | 0.09 | 6 |
| $Fe_2O_3$/TMAPS | 2.81 | 1.15 | 0.49 | 34 |
| $Fe_2O_3$/TMAPS/DNA | 3.39 | 1.15 | 0.93 | −24 |
| $Fe_2O_3$/TMAPS/DNA/$SiO_2$ | 3.12 | 1.33 | 0.64 | −24 |
| $Fe_2O_3$/TMAPS/DNA/$SiO_2$−$C_6$ | 5.13 | 1.60 | 0.66 | |

standard curves (left, triangles) and amplification curves (right) obtained from dilution series of DNA particle dispersions in water.

In order to show the advantages of magnetic separation, the particles present in 1 mL of solution were separated from an Eppendorf tube with the use of an external magnet prior to dissolution in BOE. With this procedure, 100 times more particles (and DNA) could be sampled, resulting in an ~8 cycle lower threshold $C_T$ and a consequently ~100 times lower detection limit. One part per billion (1 $\mu$g/L) of particles could be detected ($C_T \sim 24$).

To obtain tags dispersible in oils, the silica surface was further reacted with *N*-hexyltrimethoxysilane to obtain hydrophobic particles. Besides observing substantially increased compatibility with hydrophobic organic solvents, $C_6$ surface functionalization was confirmed by IR spectroscopy (Figure 3; bands at 2957, 2926, and 2858 $cm^{-1}$ indicating C−H bonds) and element microanalysis (Table 2).

The suspension stability in toluene and the corresponding particle size were assessed by photocentrifugation (LUMiSizer). The hydrodynamic particle size distribution in toluene, with a mean value of 135 nm, is displayed in Figure 1d. It was obtained from Stokes' law, assuming a particle density of 3.3 g/$cm^3$ (60 wt % $SiO_2$, 40 wt % $Fe_2O_3$; see Supporting Information for density calculation). This corresponds to a calculated particle sedimentation velocity (in the absence of additional centrifugal or magnetic forces; see Supporting Information for sedimentation velocity calculation) of $4 \times 10^{-8}$ m/s (*i.e.*, sedimenting at a rate of 4 mm per day).

The surface-functionalized particles were dispersed in toluene at various concentrations (ranging from 1 to $10^6$ $\mu$g/L), and the release of the DNA from the particles was attempted after evaporation of the toluene. However, DNA recovery was far from quantitative and differed in about 10 cycles compared to the aqueous sample. It seems that residues from the evaporated toluene were interfering with the polymerase reaction. In this scenario, magnetic separation becomes essential since it permits collection of the encapsulates and discards the supernatant instead of drying it. Additionally, bigger volumes can easily be used, increasing the amount of collectable encapsulates and recoverable DNA. As expected, *via* magnetic separation, we observed DNA amplification for all evaluated particle dilutions (from $10^4$ down to 1 $\mu$g/L = 10 ppm to 1 ppb),

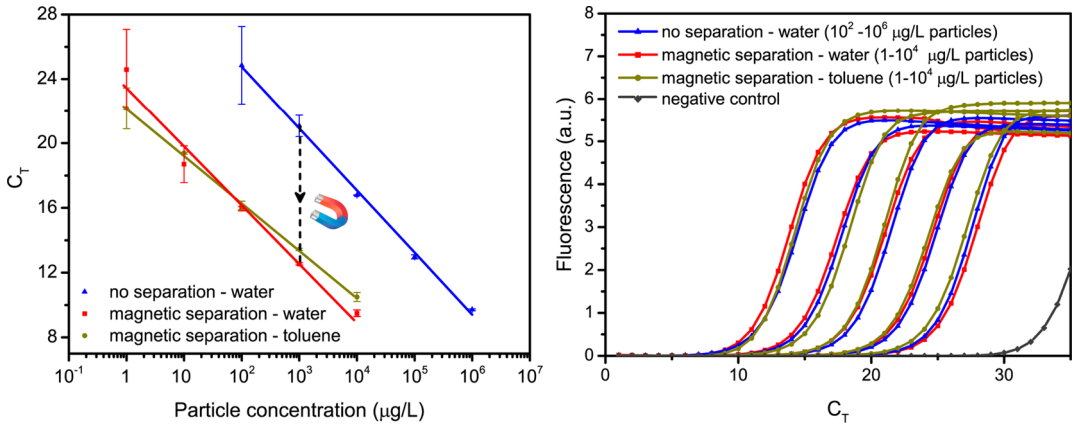


**Figure 4. Standard curves (left) and amplification curves (right) of 10-fold serial dilution of particle dispersions obtained both by direct sampling (triangles) and by magnetic separation (squares) from water and by magnetic separation from toluene (spheres). At each particle dilution, the use of magnetic separation allowed for sample preconcentration, lowering the cycle threshold $C_T$ to significantly lower values (~8 cycles, *i.e.*, 100× more concentrated).**

both in water and toluene. In all cases, the cycle threshold difference from the positive sample to the negative control was ≥7 (Figure 4). No statistical difference between the aqueous sample and the toluene sample was evident.

A proper tag must not only be dispersible in the final fluid but also be invisible, still being detectable. Therefore, it was important to assess the optical properties of particle dispersions. Visible absorption spectra and photographs of particles in toluene suspensions of different concentrations are shown in Figure 5 in comparison to pure toluene. We observed that the tags did not affect the transparency of the dispersant at concentrations below $10^3$ μg/L: particle suspensions appeared like pure toluene to the naked eye and possessed identical visible absorption spectra (max visible absorbance <0.02).

*Via* magnetic separation, we were also able to detect and quantify DNA from particle dispersions in decalin and oils. Decalin was chosen as a nonpolar high-boiling model compound. Where necessary (decalin and olive oil; see Methods), the oil was first diluted with toluene to decrease its viscosity, and the particles were separated by the use of a magnet and were washed with toluene prior to DNA release in BOE buffers. The taggant information (base sequence) was maintained during the procedure, as evidenced in the sequencing chromatograms (Sanger sequencing) in Figure 6.[28]

We tested temperature stability of the taggants in comparison to unprotected DNA. We performed the temperature treatment in water (before the hydrophobization step) because water represents the only good solvent for free DNA and encapsulated DNA. The two systems were heat treated at 95 °C for durations of up to 24 h (Figure 7a). After 4 h treatment at 95 °C, almost all of the free DNA was degraded (<0.002% remaining), while about 15% protected DNA survived. We also performed a stability test for shorter durations and

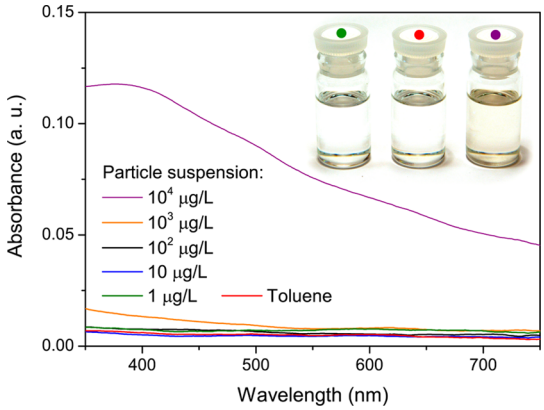


**Figure 5. Visible absorption spectra of several $Fe_2O_3$/TMAPS/DNA/$SiO_2$−$C_6$ suspensions in toluene, at different particle concentrations. A photograph insert of toluene (center) of 1 μg/L (left) and $10^4$ μg/L (right) $Fe_2O_3$/TMAPS/DNA/$SiO_2$−$C_6$ particles in toluene is included.**

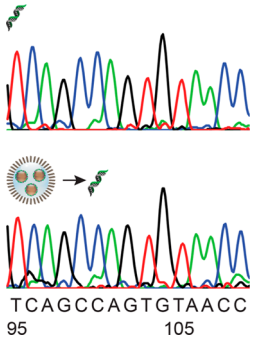


**Figure 6. Sequencing chromatograms of base 95−109 of unprocessed dsDNA sequence (top panel) and encapsulated/recovered from decalin (bottom panel).**

higher temperatures (Figure 7b) to show the increased stability of protected DNA to high level of stress. For this purpose, we used dispersions of the particles in decalin (bp = 189−191 °C), which were heat treated at temperatures between 100 and 160 °C for 30 min. For comparison, unprotected DNA solutions in water with

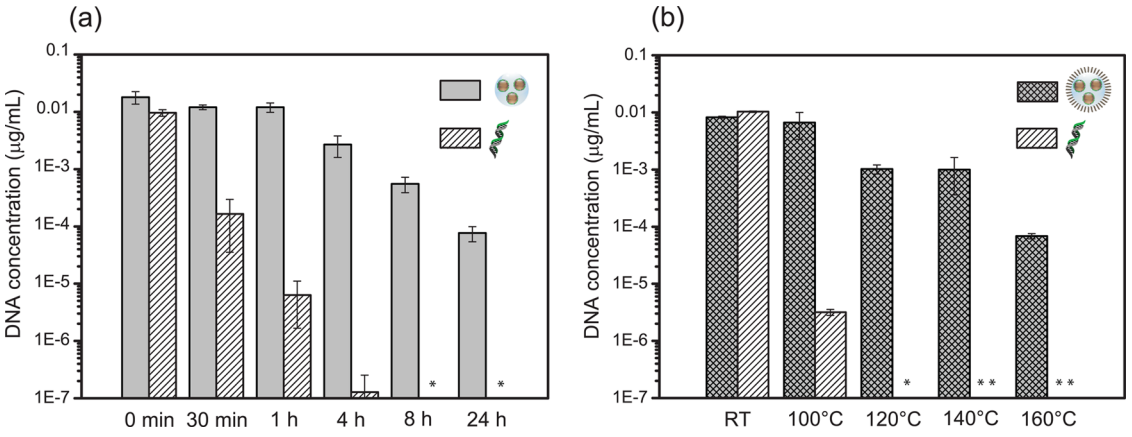


**Figure 7. (a) qPCR analysis of encapsulated DNA heat stability in water at 95 °C for durations of up to 24 h compared to that of unprotected DNA in water. Gray bars represent protected DNA, patterned bars free DNA. (b) qPCR analysis of encapsulated DNA heat stability in decalin at temperature between 100 and 160 °C (30 min treatment) compared to that of unprotected DNA in water (pressurized at 120 °C). Rhombus patterned bars represent protected DNA in decalin, line patterned bars free DNA in water. Asterisk (*) indicates data below detection limit (<$10^{-7}$ μg/mL DNA). (**) Free DNA samples were not evaluated for temperatures exceeding 120 °C due to water evaporation.**

similar DNA concentrations were also treated. About 80% DNA in $Fe_2O_3$/TMAPS/DNA/$SiO_2$−$C_6$ particles resisted the treatment at 100 °C for 30 min, conditions at which less than 0.05% unprotected DNA survived (Figure 7b). Although considerable amounts of DNA were degraded at treatments at higher temperatures, the taggants were still detectable after heating to 160 °C for 30 min (unprotected DNA was no longer detectable after heating in water to 120 °C). We additionally tested the long-term storage capability of the particles in decalin by an accelerated aging test at 65 °C for 35 days (equivalent to storage at RT for 2 years), without substantial losses (Figure S3).

To show the applicability of the magnetic taggants, we utilized gasoline as an example for a fuel, bergamot oil as an example of a cosmetic oil, and extra virgin olive oil as an example of a food grade oil. The taggants formed dispersions in all three systems. Particle sizes were assessed in gasoline and limonene (the major constituent of bergamot oil), yielding 160 and 162 nm average diameters (see Figure S4, Supporting Information; particle analysis using analytical photocentrifugation was impeded by the high viscosity and color of the olive oil). The particle size and the low concentration used suggest that sedimentation/aggregation phenomena are not significant (see calculations in Supporting Information). A dilution series over the particle concentration range of 1−100 μg/L was obtained for each oil by qPCR. Mean $C_T$ value for negative control (qPCR reaction set up with water instead of sample) was also recorded. All samples showed a clear dependence of the $C_T$ (and hence of DNA concentration) on the amount of taggant present (Figure 8). To statistically analyze qPCR results, we carried out two-sample *t* test (Supporting Information), showing for each oil that mean $C_T$ values of any pair of standard curve points recorded were significantly different if averages

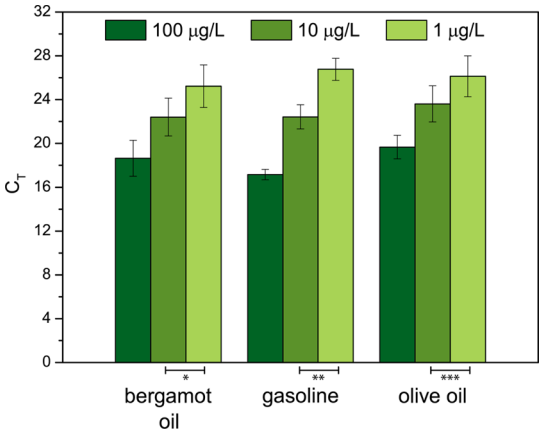


**Figure 8. qPCR analysis of DNA in oil dispersions (100, 10, and 1 μg/L $Fe_2O_3$/TMAPS/DNA/$SiO_2$−$C_6$ particles in bergamot oil, gasoline, and olive oil), showing significant $C_T$ value differences (two-sample *t* test) between oil samples at different concentrations: (*) $p < 0.05$; (**) $p < 0.001$; (***) $p < 0.1$.**

were taken from five independent samples (Figure 8 and Supporting Information for complete data set). Oil samples with merely 1 μg particles per liter were also differentiated from the negative control group to a certainty of >99.9% ($p < 0.001$ for each oil), which ensures discrimination of adulterated oil-based products. This is close to the limit of detection of the method: an additional 10-fold dilution of the oil sample would only allow differentiation from blanks to a certainty of <80% ($p > 0.2$ for $C_T \geq 30.5$), too low for a commercial use of the product. Closer differentiation of dilution would be possible if more individual samples were averaged but is limited by the intrinsic logarithmic scale of the qPCR method.

All three fluids are known objects of adulteration, and chromatographic and spectroscopic techniques are currently being used to gain insight into the modifications involved.[1,2,4,5] Results are often

unsatisfactory since it is not always possible to discriminate components added/substituted. DNA fingerprinting has been applied to identify fraudulent olive oil and/or determine its origin. However, it involves DNA extraction procedures which not always ensure enough DNA for analysis and have to be optimized based on the amount/type of PCR inhibitors present in the oil sample.[3] In contrast, the technology presented here is a universal method which could be applied to each oil type and oil sample without the need for specific optimization.

At a taggant concentration of 1 $\mu$g/L (=1 ppb) and a calculated material cost of the taggant of ~200 USD/g, the financial burden of marking a given oil with this technology is 0.02 ¢/L (calculated from chemical costs on laboratory scale, worst case; see Supporting Information for details). This is well below 0.02% of the final product value for a bulk commodity and even lower if used to mark a branded product. Furthermore, the cost is in the range of current expenses for the most accepted methods of product labeling (printing barcode on cardboard).

The taggants were designed with biocompatbility in hindsight, as both iron oxides and silica particles are considered biocompatible and a recent study showed that iron may enhance the biodegradability of silica.[43] Also, both materials are approved as food additives (amorphous silica = E551, iron oxide pigment = E172) and the Experts group on Vitamins and Minerals set a safe upper level for silicon intake at 700 mg per day.[44] Still, the use of the magnetic taggants to regulated applications in pharmaceutics, food, and cosmetics will require further toxicity testing and approval.

## CONCLUSIONS

We developed a method to produce inert taggants for oil items. They consist of hydrophobic nanoengineered particles embedding artificial dsDNA sequences. The particles have a core/shell structure, made of iron oxide and silica. The iron oxide is responsible for the magnetic properties, while the surrounding silica matrix acts as protective barrier and confers heat stability and surface functionality. DNA could be recovered from the particles upon dissolution in fluoride-containing solution and analyzed by qPCR and Sanger sequencing. The magnetic core of the particles facilitated handling and allowed for sample concentration. The magnetic tags were easily retrieved from oils, identified and quantified on a logarithmic scale: we could successfully detect them in bergamot oil, olive oil, and gasoline suspensions and statistically discriminate 10-fold dilution steps of the products. Incredibly small amounts of particles (down to 1 $\mu$g/L) and minute volumes (1 mL) were sufficient to perform authenticity tests of the oil products. Furthermore, the method is universal because it does not require procedure optimization based on oil type.

## METHODS

**$Fe_2O_3$/TMAPS/DNA/$SiO_2$–$C_6$ Particle Synthesis.** $Fe_2O_3$ particles were synthetized by conventional co-precipitation of $Fe^{2+}/^{3+}$ ions ($Fe^{2+}/Fe^{3+}$ = 1:2) under alkaline conditions. Four grams of $FeCl_2 \cdot 4H_2O$ (Aldrich, 99%) and 10.8 g of $FeCl_3 \cdot 6H_2O$ (Aldrich, 98%) were dissolved in 50 mL of distilled water. The solution was added dropwise into 500 mL of a 1 M $NH_4OH$ (prepared from Sigma Aldrich, 25%) solution under vigorous stirring at room temperature. The obtained particles were washed five times and stored in water at a concentration of ~50 mg/mL.

The prepared magnetic particles were functionalized with ammonium groups using *N*-trimethoxysilylpropyl-*N*,*N*,*N*-trimethylammonium chloride (TMAPS, 50% in MeOH, ABCR GmbH).[14,28,42] Ten microliters of TMAPS was added to 1 mL of particle suspension in isopropyl alcohol (~50 mg/mL), and the mixture was stirred overnight (900 rpm) at room temperature. Particles were washed three times and stored in isopropyl alcohol at ~50 mg/mL.

The dsDNA (5′-ATT CAT GCG ACA GGG GTA AGA CCA TCA GTA GTA GGG ATA GTG CCA AAC CTC ACT CAC CAC TGC CAA TAA GGG GTC CTT ACC TGA AGA ATA AGT GTC AGC CAG TGT AAC CCG AT-3′, purchased by Microsynth AG) was adsorbed on the particles by mixing 1 mL of a 16 $\mu$g/mL DNA solution in water with 15 $\mu$L of particle suspension, followed by three washing cycles and redispersion in water (0.5 mL).

An additional layer of TMAPS was adsorbed onto the particle surface before growing $SiO_2$ by using tetraethoxysilane (TEOS, ≥99%, Aldrich) as Si source.[14,28] One microliter of TMAPS was added to the particle dispersion, which was then vortexed before adding 1 $\mu$L of TEOS. The mixture was stirred (900 rpm) for 4 h at room temperature, and then additional 8 $\mu$L of TEOS was added. The reaction was run for 4 days and stirred at 900 rpm.

$C_6$ functionalization was achieved by conducting hydrolysis of *N*-hexyltrimethoxysilane according to the following procedure. $Fe_2O_3$/TMAPS/DNA/$SiO_2$ particles were redispersed in ethanol (260 $\mu$L, ~4 mg/mL). Forty microliters of $NH_4OH$ (Sigma Aldrich, 25%) was added, and the dispersion was stirred (900 rpm) for 30 min at 40 °C. A solution consisting of 100 $\mu$L of *N*-hexyltrimethoxysilane (TCI, >96%) and 50 $\mu$L of ethanol was then added. The mixture was stirred overnight at 40 °C. The particles were washed three times and stored in toluene (100 $\mu$L, 10 mg/mL).

**DNA Recovery.** Encapsulated dsDNA was recovered using a buffered oxide etch solution ($NH_4FHF/NH_4F$, 0.23 g of $NH_4FHF$ + 0.19 g of $NH_4F$ in 10 mL of water) prepared and handled as described in Paunescu *et al.*[28] Since $C_6$-functionalized particles are highly hydrophobic and the etching solution is aqueous, more time was required for their complete dissolution than the time needed to dissolve the nonfunctionalized ones (few minutes).

**qPCR Standard Curves.** Standard curves were obtained from 10-fold dilution series (in water for unfunctionalized particles, in toluene, bergamot oil, gasoline, and extra virgin olive oil for particles bringing $C_6$ modification) of the original particle dispersions. For comparison, both curves without and *via* magnetic separation were produced. *Without magnetic separation:* 300 $\mu$L of diluted buffered oxide etch (1:100) was added to 10 $\mu$L of particle dispersion at each dilution to dissolve the particles. When toluene was the dispersant, the sample was dried at 45 °C (Concentrator plus, Eppendorf AG) for 15 min before adding the etching solution. The solution was directly analyzed by qPCR. *With magnetic separation:* 1 mL of particle dispersion was placed in a magnetic separator and left to allow for complete particle separation. Olive oil suspension was diluted with

toluene (1 mL of oil + 1 mL of toluene) to facilitate separation. Particles collected from oil suspensions were washed once with toluene. Again, drying (3 min) was necessary to remove residual toluene. Then, 300 $\mu$L of diluted buffered oxide etch was added as before, and qPCR was performed. A standard qPCR protocol (Roche LightCycler 96) was used, with the following primers sequences: 5′-ATT CAT GCG ACA GGG GTA AG-3′ (forward primer) and 5′-ATC GGG TTA CAC TGG CTG AC-3 (reverse primer), purchased from Microsynth AG. Experiments with water and toluene particle suspensions were performed in triplicate ($n$ = 3) and repeated twice, with similar results, to determine both qPCR analysis reproducibility and reproducibility of the experiments. In the case of the oils, five samples for each taggant concentration considered were analyzed, each assayed by qPCR six times ($n$ = 30). Each qPCR reaction was assessed against a negative control, which contains water instead of sample DNA. Data are provided as mean $C_T$ value ± standard deviation.

**DNA Absolute Quantification.** Sample absolute quantification was accomplished using a standard curve (Figure S2 in the Supporting Information), generated from DNA samples of known concentration (determined by Qubit dsDNA HS assay, Invitrogen). Any unknown sample concentration was then determined by interpolation from this curve.

**Thermal Stability.** For comparison, both encapsulated and free dsDNA were heat treated. *Free DNA*: 100 $\mu$L of dsDNA in water (0.08 $\mu$g/mL) was treated at 95 °C for a duration up to 24 h (two samples per time point, each analyzed in triplicate by qPCR) and at various temperatures (100 and 120 °C) for 30 min (two samples per temperature, each analyzed in duplicate). *Protected DNA*: 100 $\mu$L of a $10^6$ $\mu$g/L $Fe_2O_3$/TMAPS/DNA/$SiO_2$ particle dispersion in water was heat treated at 95 °C for periods of time up to 24 h (two samples per time point, each analyzed in triplicate). Then, 300 $\mu$L of diluted buffered oxide etch (1:100) was added to 10 $\mu$L of treated particle dispersion, and the obtained DNA solution was analyzed and quantified by qPCR. One hundred microliters of a $10^5$ $\mu$g/L $Fe_2O_3$/TMAPS/DNA/$SiO_2$−$C_6$ particle dispersion in decalin (mixture of *cis* + *trans*, 98%, Sigma Aldrich) was heat treated at temperatures between 100 and 160 °C for 30 min (two samples per temperature, each analyzed in duplicate). After treatment, the dispersion (100 $\mu$L) was diluted with toluene (900 $\mu$L) to reduce the viscosity, before separating the particles by magnetic means. The separated particles were dried for 3 min at 45 °C and dissolved using 300 $\mu$L of 1:100 BOE. The DNA solution was directly analyzed and quantified by qPCR.

Data and error bars represent concentration mean values and standard deviations obtained.

**Sanger Sequencing.** Particles were separated from 100 $\mu$L of $10^6$ $\mu$g/L dispersion in decalin by magnetic means. After a wash with toluene, particles were dissolved in 100 $\mu$L of buffered oxide etch. DNA solution was then purified (QIAquick PCR purification kit) and sequenced. DNA was sequenced in the direction 5′-3′ with the primer 5′-CAG GGG TAA GAC CAT CAG-3′ (Microsynth AG).

*Conflict of Interest:* The authors declare the following competing financial interest(s): Two authors declare employment and personal financial interest. R.N.G. and W.J.S. declare financial interest in the form of a patent application on DNA encapsulation licenced to TurboBeads Llc, of which R.N.G. and W.J.S. are a shareholder. M.P. and D.P. have no competing financial interests.

*Acknowledgment.* We thank the EU-ITN network Mag(net)icFun (PITN-GA-2012-290248) and the Swiss National Science Foundation (No. 200021-150179) for financial support, and Hanspeter Hächler for magnetic hysteresis measurements.

*Supporting Information Available:* Material characterization methods; particle density calculation; sedimentation velocity calculation; particle aggregation time calculation; independent two-sample $t$ test; TEM micrographs of pristine $Fe_2O_3$ and of $Fe_2O_3$/TMAPS/DNA/$SiO_2$ particles; standard curve for DNA quantification; long-term DNA stability; particle size distributions of $Fe_2O_3$/TMAPS/DNA/$SiO_2$-$C_6$ particles in toluene, gasoline, and limonene; cost analysis. This material is available free of charge *via* the Internet at http://pubs.acs.org.

## REFERENCES AND NOTES

1. Oliveira, F. C. C.; Brandão, C. R. R.; Ramalho, H. F.; da Costa, L. A. F.; Suarez, P. A. Z.; Rubim, J. C. Adulteration of Diesel/Biodiesel Blends by Vegetable Oil As Determined by Fourier Transform (FT) Near Infrared Spectrometry and FT-Raman Spectroscopy. *Anal. Chim. Acta* **2007**, *587*, 194–199.
2. Pereira, R. C. C.; Skrobot, V. L.; Castro, E. V. R.; Fortes, I. C. P.; Pasa, V. M. D. Determination of Gasoline Adulteration by Principal Components Analysis—Linear Discriminant Analysis Applied to FTIR Spectra. *Energy Fuels* **2006**, *20*, 1097–1102.
3. Woolfe, M.; Primrose, S. Food Forensics: Using DNA Technology To Combat Misdescription and Fraud. *Trends Biotechnol.* **2004**, *22*, 222–226.
4. Tay, A.; Singh, R. K.; Krishnan, S. S.; Gore, J. P. Authentication of Olive Oil Adulterated with Vegetable Oils Using Fourier Transform Infrared Spectroscopy. *Lebensm.-Wiss. Technol., Food Sci. Technol.* **2002**, *35*, 99–103.
5. Konig, W. A.; Fricke, C.; Saritas, Y.; Momeni, B.; Hohenfeld, G. Adulteration or Natural Variability? Enantioselective Gas Chromatography in Purity Control of Essential Oils. *J. High Resolut. Chromatogr.* **1997**, *20*, 55–61.
6. Bryce, D. R. Magnetic Document Validator Employing Remanence and Saturation Measurements. U.S. 5,068,519, November 26, 1991.
7. McGrew, S. P. Quantum Dot Security Device and Method. U.S. 6,692,031 B2, February 17, 2004.
8. Small, L. D.; Highberger, G. Thermochromic Ink Formulations, Nail Lacquer and Methods of Use. U.S. 5,997,849, December 7, 1997.
9. Welle, R. P. Isotopic Taggant Method and Composition. U.S. 5,760,394, June 2, 1998.
10. Shchegolikhin, A. N.; Lazareva, O. L.; Mel'nikov, V. P.; Ozeretski, V. Y.; Small, L. D. Raman-Active Taggants and Their Recognition. U.S. 6,610,351 B2, August 26, 2003.
11. Kydd, P. H. Polypeptides as Chemical Tagging Materials. U.S. 4,441,943, April 10, 1984.
12. Lebacq, P. Method and Apparatus for High Security Crypto-Marking for Protecting Valuable Objects. U.S. 5,139,812, August 18, 1992.
13. Slater, J. H.; Minton, J. E. Method of Marking a Liquid. U.S. 5,643,728, July 1, 1997.
14. Paunescu, D.; Fuhrer, R.; Grass, R. N. Protection and Deprotection of DNA: High Temperature Stability of Nucleic Acid Barcodes for Polymer Labeling. *Angew. Chem., Int. Ed.* **2013**, *52*, 4269–4272.
15. Lu, C.-H.; Willner, B.; Willner, I. DNA Nanotechnology: From Sensing and DNA Machines to Drug-Delivery Systems. *ACS Nano* **2013**, *7*, 8320–8332.
16. Pinheiro, A. V.; Han, D.; Shih, W. M.; Yan, H. Challenges and Opportunities for Structural DNA Nanotechnology. *Nat. Nanotechnol.* **2011**, *6*, 763–772.
17. Zhang, Z.; Balogh, D.; Wang, F.; Sung, S. Y.; Nechushtai, R.; Willner, I. Biocatalytic Release of an Anticancer Drug from Nucleic-Acids-Capped Mesoporous $SiO_2$ Using DNA or Molecular Biomarkers as Triggering Stimuli. *ACS Nano* **2013**, *7*, 8455–8468.
18. Seeman, N. C. Structural DNA Nanotechnology: Growing Along with Nano Letters. *Nano Lett.* **2010**, *10*, 1971–1978.
19. Niemeyer, C. M. Self-Assembled Nanostructures Based on DNA: Towards the Development of Nanobiotechnology. *Curr. Opin. Chem. Biol.* **2000**, *4*, 609–618.
20. Ke, Y.; Ong, L. L.; Shih, W. M.; Yin, P. Three-Dimensional Structures Self-Assembled from DNA Bricks. *Science* **2012**, *338*, 1177–1183.
21. Auyeung, E.; Li, T. I. N. G.; Senesi, A. J.; Schmucker, A. L.; Pals, B. C.; de la Cruz, M. O.; Mirkin, C. A. DNA-Mediated Nanoparticle Crystallization into Wulff Polyhedra. *Nature* **2014**, *505*, 73–77.
22. Davila-Ibanez, A. B.; Salgueirino, V.; Martinez-Zorzano, V.; Mariño-Fernández, R.; García-Lorenzo, A.; Maceira-Campos, M.; Muñoz-Ubeda, M.; Junquera, E.; Aicart, E.; Rivas, J.; *et al.* Magnetic Silica Nanoparticle Cellular Uptake and Cytotoxicity Regulated by Electrostatic Polyelectrolytes—DNA Loading at Their Surface. *ACS Nano* **2011**, *6*, 747–759.

23. Ruiz-Hernández, E.; Baeza, A.; Vallet-Regí, M. Smart Drug Delivery through DNA/Magnetic Nanoparticle Gates. *ACS Nano* **2011**, *5*, 1259–1266.
24. Choy, J. H.; Oh, J. M.; Park, M.; Sohn, K. M.; Kim, J. W. Inorganic-Biomolecular Hybrid Nanomaterials as a Genetic Molecular Code System. *Adv. Mater.* **2004**, *16*, 1181–1184.
25. Park, D. H.; Kim, J. E.; Oh, J. M.; Shul, Y. G.; Choy, J. H. DNA Core@ Inorganic Shell. *J. Am. Chem. Soc.* **2010**, *132*, 16735–16736.
26. Church, G. M.; Gao, Y.; Kosuri, S. Next-Generation Digital Information Storage in DNA. *Science* **2012**, *337*, 1628–1628.
27. Goldman, N.; Bertone, P.; Chen, S. Y.; Dessimoz, C.; LeProust, E. M.; Sipos, B.; Birney, E. Towards Practical, High-Capacity, Low-Maintenance Information Storage in Synthesized DNA. *Nature* **2013**, *494*, 77–80.
28. Paunescu, D.; Puddu, M.; Soellner, J. O. B.; Stoessel, P. R.; Grass, R. N. Reversible DNA Encapsulation in Silica To Produce ROS-Resistant and Heat-Resistant Synthetic DNA 'Fossils'. *Nat. Protoc.* **2013**, *8*, 2440–2448.
29. Lindahl, T. Instability and Decay of the Primary Structure of DNA. *Nature* **1993**, *362*, 709–715.
30. He, X. X.; Wang, K. M.; Tan, W. H.; Liu, B.; Lin, X.; He, C. M.; Li, D.; Huang, S. S.; Li, J. Bioconjugated Nanoparticles for DNA Protection from Cleavage. *J. Am. Chem. Soc.* **2003**, *125*, 7168–7169.
31. Radu, D. R.; Lai, C. Y.; Jeftinija, K.; Rowe, E. W.; Jeftinija, S.; Lin, V. S. Y. A Polyamidoamine Dendrimer-Capped Mesoporous Silica Nanosphere-Based Gene Transfection Reagent. *J. Am. Chem. Soc.* **2004**, *126*, 13216–13217.
32. Zelikin, A. N.; Becker, A. L.; Johnston, A. P. R.; Wark, K. L.; Turatti, F.; Caruso, F. A General Approach for DNA Encapsulation in Degradable Polymer Microcapsules. *ACS Nano* **2007**, *1*, 63–69.
33. Smith, S.; Morin, P. A. Optimal Storage Conditions for Highly Dilute DNA Samples: A Role for Trehalose as a Preserving Agent. *J. Forensic Sci. Soc.* **2005**, *50*, 1101–1108.
34. Rajendram, D.; Ayenza, R.; Holder, F. M.; Moran, B.; Long, T.; Shah, H. N. Long-Term Storage and Safe Retrieval of DNA from Microorganisms for Molecular Analysis Using FTA Matrix Cards. *J. Microbiol. Methods* **2006**, *67*, 582–592.
35. Yang, H.; Zheng, K.; Zhang, Z.; Shi, W.; Jing, S.; Wang, L.; Zheng, W.; Zhao, D.; Xu, J.; Zhang, P. Adsorption and Protection of Plasmid DNA on Mesoporous Silica Nanoparticles Modified with Various Amounts of Organosilane. *J. Colloid Interface Sci.* **2012**, *369*, 317–322.
36. Kapusuz, D.; Durucan, C. Synthesis of DNA-Encapsulated Silica Elaborated by Sol−Gel Routes. *J. Mater. Res.* **2013**, *28*, 175–184.
37. Lu, A. H.; Salabas, E. L.; Schuth, F. Magnetic Nanoparticles: Synthesis, Protection, Functionalization, and Application. *Angew. Chem., Int. Ed.* **2007**, *46*, 1222–1244.
38. Aguilar-Arteaga, K.; Rodriguez, J. A.; Barrado, E. Magnetic Solids in Analytical Chemistry: A Review. *Anal. Chim. Acta* **2010**, *674*, 157–165.
39. Hao, R.; Xing, R. J.; Xu, Z. C.; Hou, Y. L.; Gao, S.; Sun, S. H. Synthesis, Functionalization, and Biomedical Applications of Multifunctional Magnetic Nanoparticles. *Adv. Mater.* **2010**, *22*, 2729–2742.
40. Sharma, A. N.; Luo, D.; Walter, M. T. Hydrological Tracers Using Nanobiotechology: Proof of Concept. *Environ. Sci. Technol.* **2012**, *46*, 8928–8936.
41. Wu, W.; He, Q.; Jiang, C. Magnetic Iron Oxide Nanoparticles: Synthesis and Surface Functionalization Strategies. *Nanoscale Res. Lett.* **2008**, *3*, 397–415.
42. Liu, B.; Yao, Y.; Che, S. Template-Assisted Self-Assembly: Alignment, Placement, and Arrangement of Two-Dimensional Mesostructured DNA−Silica Platelets. *Angew. Chem., Int. Ed.* **2013**, *52*, 1–6.
43. Mitchell, K. K. P.; Liberman, A.; Kummel, A. C.; Trogler, W. C. Iron(III)-Doped, Silica Nanoshells: A Biodegradable Form of Silica. *J. Am. Chem. Soc.* **2012**, *134*, 13997–14003.
44. Aguilar, F.; Charrondiere, U. R.; Dusemund, B.; Galtier, P.; Gilbert, J.; Gott, D. M.; Grilli, S.; Guertler, R.; Kass, G. E. N.; Koenig, J.; *et al.* Calcium Silicate and Silicon Dioxide/Silicic Acid Gel Added for Nutritional Purposes to Food Supplements. *EFSA J.* **2009**, *1132*, 1–24.